Hindawi
Journal of Chemistry
Volume 2018, Article ID 2041812, 9 pages
https://doi.org/10.1155/2018/2041812

Research Article

Optimization to Hydrothermal Liquefaction of Low Lipid Content Microalgae *Spirulina* sp. Using Response Surface Methodology

Xuan Wei[1,2] **and Dengfei Jie**[3]

[1]*College of Mechanical and Electronic Engineering, Fujian Agriculture and Forestry University, Fuzhou 350002, China*
[2]*Engineering Research Center for Modern Agricultural Equipment, Fujian Agriculture and Forestry University, Fuzhou 350002, China*
[3]*College of Engineering, Huazhong Agricultural University, Wuhan 430070, China*

Correspondence should be addressed to Dengfei Jie; dfjie@mail.hzau.edu.cn

Received 3 August 2017; Accepted 24 January 2018; Published 21 May 2018

Academic Editor: Albert Demonceau

The production and nature of the biocrude obtained from *Spirulina* sp. by hydrothermal liquefaction (HTL) technology is focused in this investigation. Our aim is to evaluate the interaction of different factors on the bio-oil production through HTL using microalgae that contains relatively low lipid content and high protein. Optimization of three key parameters—concentration (mass of algae per mass of solvent), reaction temperature, and holding time—was carried out by response surface methodology (RSM). In this work, we used central composite design to conduct the experiment process. Graphical response surface and contour plots were used to locate the optimum point. The final results showed that the optimum concentration, temperature, and holding time were 10.5%, 357°C, and 37 min, respectively. Under the optimum conditions established, yield of the biocrude (41.6 ± 2.2%) was experimentally obtained using the fresh microalgae. This study showed the potential of bio-oil production of *Spirulina* sp. by HTL technology, but it still needs more improvement of the biocrude for utilization.

1. Introduction

Microalgae, which could fast convert CO_2 into biomass, have got an increasing interesting role in biofuel production [1]. They are considered more photosynthetically efficient than any other energy plants [2].

Microalgae have shown great potential to produce a wide variety of fuel products in present studies [3, 4]: (1) hydrogen (H_2) via direct and indirect biophotolysis [5], (2) biodiesel through transesterification [6], (3) biomethane via anaerobic digestion [7], (4) bioethanol by fermentation [8], and (5) bio-oil via thermochemical conversion [9].

Usually, microalgae contain the lipid in the range of 20–50% [10]. The lipid content is dependent upon strain and growth conditions [11]. After solvent extraction or physical extraction, these lipids of microalgae can then be further transesterified to biodiesels. One of the problems of this approach is that the wet aquatic biomass requires drying before it can be processed [12]. Hydrothermal liquefaction is one of the alternatives being increasingly considered, especially at low temperatures and pressures near the water critical pressure [13]. Wet microalgae with high water content could be converted into crude bio-oil by thermally and hydrolytically decomposing the biomacromolecules such as protein and lipid into smaller compounds. The biocrude is an energy dense product that can potentially be used as a substitute for petroleum crudes [14]. Some reports showed that hydrothermal liquefaction could be widely applied to various microalgae as the oil yield usually exceeds the crude fat content of microalgae [15].

Some of the most productive microalgae in terms of biomass production are lower in lipid and contain larger amounts of protein and carbohydrate [16]. Growing these algae for biodiesel is unlikely to be economical, and the alternative-processing routes would be advantageous such as *Spirulina*. The *Spirulina* industry in China is developing

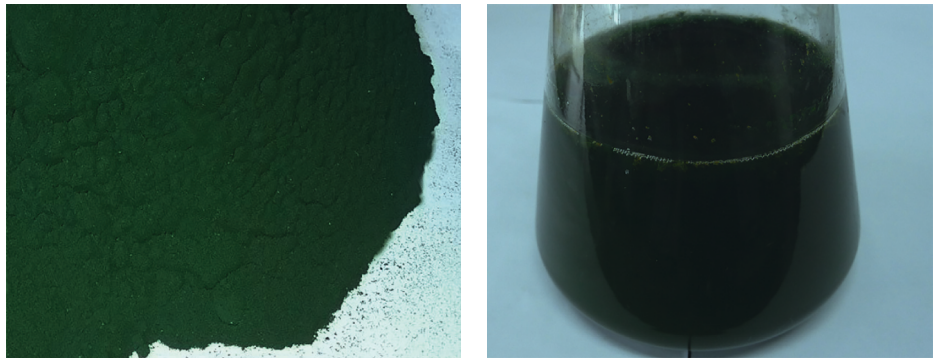

(a) (b)

Figure 1: *Spirulina* sp. powder and cultured *Spirulina* sp.

rapidly as a national strategic programme [17]. By the mid-1990s, China has become the biggest country in *Spirulina* production in the world. Just in 2009, 3,500 t (dw) of *Spirulina* have been produced [18]. The supply of *Spirulina* as the functional food has much exceeded the demand. Some studies showed the possibility of producing bio-oil using *Spirulina* by liquefaction technology [19–22]. If bio-oil is to be obtained efficiently from mass-cultivated *Spirulina* by liquefaction, this will be one of the both promising methods for energy production and one of the *Spirulina* consumption.

To date, there is still lack of the studies about the interaction of multifactors on bio-oil production using *Spirulina*. This work focuses on the optimization of hydrothermal liquefaction condition of *Spirulina* sp. using response surface methodology (RSM). The influences of process variables containing feedstock concentration, temperature, and holding time have been studied. We hope to evaluate the maximum production rate and further analyze the characteristic of biocrude by using the wet microalgae as the feedstock under the optimal condition.

2. Materials and Methods

2.1. Strains and Culture Media. The *Spirulina* sp. strain was bought from Freshwater Algae Culture Collection at the Institute of Hydrobiology (FACHB-collection). Strains were cultured for three weeks at 25°C with a continuous illumination of 120 μ·mol·m^{-2}s^{-1} in *Spirulina* medium. Per 1 liter, *Spirulina* medium contained 13.61 g of $NaHCO_3$, 4.03 g of Na_2CO_3, 0.50 g of K_2HPO_4, 2.50 g of $NaNO_3$, 1.00 g of K_2SO_4, 1.00 g of NaCl, 0.20 g of $MgSO_4{\cdot}7H_2O$, 0.04 g of $CaCl_2{\cdot}2H_2O$, 0.01 g of $FeSO_4{\cdot}7H_2O$, and 1 mL of trace metal mix A_5. The trace metal mix A_5 contained 2.86 g of H_3BO_3, 1.81 g of $MnCl_2{\cdot}4H_2O$, 0.222 g of $ZnSO_4{\cdot}7H_2O$, 0.039 g of $NaMoO_4{\cdot}2H_2O$, 0.079 g of $CuSO_4{\cdot}5H_2O$, and 0.049 g of $Co(NO_3)_2{\cdot}6H_2O$ in 1 L of distilled water.

The freeze-dried *Spirulina* sp. powder was got from a local microalgae cultured farm. It was kept in dryer at −4°C. We measured the moisture of the fresh *Spirulina* sp. after reducing most of the water by centrifugation, and then, we diluted the sludge into the specific concentration after the optimization calculation. Meanwhile, the lipid and protein content of *Spirulina* sp. powder and fresh (Figure 1) were measured by the Soxhlet extraction method and Dumas combustion method, respectively.

2.2. Elements Analyses and Higher Heating Value (HHV) Estimate. The basic elements of the biomass are listed in Table 1. C, H, N, and S contents of the biomass were measured using an elemental analyzer (Flash EA 1112 series, CE Instruments, Italy). All measurements were repeated in triplicate, and a mean value was reported.

Estimation of HHV from the elemental composition of fuel is one of the basic steps in performance modeling and calculations on thermal systems [23]. As HHV is an important fuel property which defines the energy content of the fuel, we calculated the biomass and biocrude by the following equations, respectively [24, 25]:

$$\mathrm{HHV}\left(\mathrm{MJ}\cdot\mathrm{kg}^{-1}\right) = 0.3383 * \mathrm{C} + 1.443 * \left(\mathrm{H} - \left(\frac{\mathrm{O}}{8}\right)\right) + 0.0942 * \mathrm{S}, \quad (1)$$

$$\mathrm{HHV}\left(\mathrm{MJ}\cdot\mathrm{kg}^{-1}\right) = 0.352\mathrm{C} + 0.944\mathrm{H} + 0.105(\mathrm{S}-\mathrm{O}), \quad (2)$$

where C, H, O, and S are the weight percentages of carbon, hydrogen, oxygen, and sulfur, respectively.

2.3. Apparatus and Experimental Procedure. We applied central composite design of three key factors and five levels to simulate our experiment (Design-expert, V8.0, Stat-ease, Inc., USA). 374°C is the critical temperature, a dramatic increase of biomass degradation rate could appear near this critical point owing to the hydrolyze capability of water [26]. And after some single factor trials, the parameters were set like in Table 2. Finally, we obtained sixty biocrude samples from each of the conversion process that were triple duplicated.

The hydrothermal liquefaction was performed in a reactor (2 L, Parr, USA) at heating rate of the reactor approximately 2°C·min^{-1}. In each case, different weight of microalgae was mixed in deionized water. Microalgae were

Table 1: Elemental analysis and HHV estimate.

Sample	Elemental compositions					HHV (MJ·kg^{-1})	Lipid (wt.%)	Protein (wt.%)
	C	H	N	S	O			
Powder	44.4	6.7	9.8	0.69	38.3	18.1	7.8%	63.7%
Fresh	43.3	6.5	10.8	0.54	38.8	17.4	8.1%	64.2%

Table 2: Experimental factors and the levels.

Factors	Encoding of the variables (x_i) and level				
	−1.682	−1	0	1	1.682
x_1 concentration (%)	7.5	9.5	12.5	15.5	17.5
x_2 temperature (°C)	315	327	345	363	375
x_3 time (min)	20	28	40	52	60

added into the reactor premixed as slurry. Then, the reactor vessel was sealed and nitrogen was introduced to purge the residual air. The microalgae slurry was stirred during the whole process. The speed of magnetic stir bar was set at 100 rpm. Meanwhile, the stir was cooled down by the condense water. The reaction started by heating the autoclave with an electric furnace. After heating the autoclave up to the required temperature, the temperature was maintained constant for the desired holding time, and then, the autoclave was allowed to cool to the room temperature.

2.4. Yield. After the conversion finished, we opened the reactor and dumped the reaction mixture into a beaker. The reactor and stir bar were washed with trichloromethane, and then, they were poured into the beaker too (Figure 2). And then, the solid residue was separated by the glass microfiber filter. The trichloromethane together with the reaction solvent was separated from the water-insoluble substance, and then, the trichloromethane in the mixture was evaporated using the rotary evaporator (RV 10 digital, IKA, Staufen, German) at 60°C under a vacuum condition.

The material remaining in the flask was the biocrude. The weight of biocrude was calculated by using the overall weight of the remaining materials after evaporation subtracting the initial trichloromethane-soluble substrate. The yield of biocrude is determined on a dry basis using the following equation:

$$\text{Yield of biocrude (wt.\%)} = \frac{\text{weight of biocrude}}{\text{weight of algae powder}} \times 100\%. \quad (3)$$

2.5. FT-IR Analysis. Infrared (IR) spectra for biocrude samples were acquired using a FT-IR spectrometer (4100, JASCO Inc., Tokyo, Japan) to determine the main organic components based on the peaks of the functional groups present. The measurement wavenumber range is 7,800 to 350 cm^{-1} and resolution is 4 cm^{-1}, controlled by JASCO's exclusive Spectra Manager™ cross-platform software.

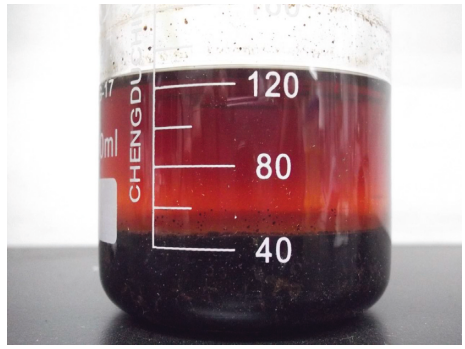

Figure 2: The reaction mixture with trichloromethane.

2.6. Constituent Analysis of the Fresh Biomass-Based Bio-Oil. The biocrude is analyzed by GC/MS on an Agilent 6890N GC/5975B MSD. A volume of 0.5 mL was injected for each sample, and the inlet temperature and split ratio are 300°C and 3 : 1, respectively. Two minutes solvent delay was set to protect the filament. The column was initially held at 40°C for 4 min. The temperature was ramped to 300°C at 4°C·min^{-1} and held isothermally for 4 min, giving a total runtime of about 60 min. Helium flowing at 3 mL·min^{-1} served as the carrier gas. NIST Mass Spectra Database was used for compound identification.

3. Results and Discussion

3.1. Sample Workup and Analysis. The optimization process was carried out to determine the optimum value of bio-oil yield using the Design Expert 8.0 software. The biocrude is a dark viscous liquid. Table 3 shows the yield of each experiment. The yield of biocrude was in the range of 37.2–44.4% and the average was 40.9%. Table 4 shows that the HHV was in the range of 26.7–36.0% and the average was 32.0 MJ·kg^{-1}. The HHV are much higher than the feedstock. The oxygen content of microalgal biocrude in our study was a little higher than in some other microalgal liquefaction studies [20, 27]. The sulfur content of microalgal bio-oil was less than 1% in all cases.

We used the Design Expert software to analyze the experimental results by multiple regressions fitting analysis. Following is the quadric multiple regression equation of yield:

$$Y = -580.64 + 6.28x_1 + 3.18x_2 + 1.33x_3 - 0.0107x_1x_2 + 0.0021x_1x_3 - 0.0013x_2x_3 - 0.12x_1^2 - 0.0042x_2^2 - 0.012x_3^2. \quad (4)$$

Table 3: Experimental design and the results.

	Variables			Volume (mL)	Maximum pressure (MPa)	Yield (%)
	x_1	x_2	x_3			
1	1	1	1	80	12.03	40.8 ± 0.88
2	1	1	−1	100	11.89	43.5 ± 1.21
3	1	−1	1	150	11.33	38.1 ± 1.06
4	1	−1	−1	150	11.12	38.9 ± 1.13
5	−1	1	1	80	11.91	38.7 ± 0.95
6	−1	1	−1	100	11.78	40.3 ± 0.90
7	−1	−1	1	150	10.98	37.5 ± 1.15
8	−1	−1	−1	150	10.62	38.8 ± 0.95
9	1.682	0	0	120	11.34	43.3 ± 1.35
10	−1.682	0	0	120	11.57	38.2 ± 1.11
11	0	1.682	0	80	12.75	42.6 ± 1.35
12	0	−1.682	0	180	10.91	37.2 ± 0.72
13	0	0	1.682	120	11.86	38.8 ± 0.74
14	0	0	−1.682	120	11.12	39.2 ± 0.86
15	0	0	0	120	11.32	43.6 ± 1.23
16	0	0	0	120	11.51	44.2 ± 1.02
17	0	0	0	120	11.33	43.9 ± 0.99
18	0	0	0	120	11.36	43.3 ± 1.06
19	0	0	0	120	11.48	44.4 ± 1.56
20	0	0	0	120	11.22	42.9 ± 0.89

x_1, concentration; x_2, temperature; x_3, holding time.

Table 4: The element analysis of each sample.

	Elements (%)					HHV ($MJ \cdot kg^{-1}$)
	C	H	N	S	O	
1	69.47	8.82	6.75	0.68	14.28	33.8
2	68.13	8.68	7.05	0.57	15.57	32.8
3	69.89	8.97	7.35	0.69	13.10	34.3
4	63.64	8.26	6.94	0.77	20.40	29.9
5	72.37	9.28	7.16	0.56	10.64	36.0
6	68.51	8.70	6.93	0.56	15.30	33.0
7	66.63	8.56	7.17	0.71	16.92	31.9
8	62.49	7.91	6.93	0.49	22.18	28.6
9	65.20	8.53	6.64	0.65	18.98	31.0
10	64.07	8.08	6.67	0.54	20.64	29.7
11	65.96	8.21	6.64	0.55	18.64	30.9
12	59.93	7.59	6.60	0.52	25.35	26.7
13	69.64	8.87	7.02	0.74	13.73	34.0
14	65.27	8.37	6.96	0.56	18.84	30.8
15	67.64	8.76	6.85	0.64	16.11	32.7
16	68.08	8.68	6.88	0.63	15.72	32.8
17	67.51	8.71	6.84	0.58	16.36	32.5
18	67.91	8.78	6.87	0.61	15.83	32.9
19	68.25	8.58	6.89	0.65	15.62	32.7
20	67.66	8.69	6.87	0.60	15.90	32.6

Table 5: Test of significance of the quadratic equation coefficient and ANOVA for the response surface quadratic model.

Source*	Sum of squares	df	Mean square	F value	p value prob. > F
Model	120.41	9	13.38	23.02	<0.0001
x_1	15.56	1	15.56	26.77	0.0004
x_2	26.66	1	26.66	45.87	<0.0001
x_3	3.66	1	3.66	6.3	0.0309
x_1x_2	2.64	1	2.64	4.55	0.0587
x_1x_3	0.045	1	0.045	0.077	0.7865
x_2x_3	0.6	1	0.6	1.04	0.3316
x_1^2	16.45	1	16.45	28.3	0.0003
x_2^2	27	1	27	46.46	<0.0001
x_3^2	41.01	1	41.01	70.57	<0.0001
Residual	5.81	10	0.58	—	—
Lack of fit	4.24	5	0.85	2.70	0.1502
Pure error	1.57	5	0.31	—	—
Cor. total	126.22	19	—	—	—

*x_1, concentration; x_2, temperature; x_3, holding time. The determination coefficient (R^2) of the regression model is 0.9540.

After that, we carried on a significance test of the regression equation. From Table 5, we can see that first degree terms of temperature and concentration are very significant ($p < 0.01$), the holding time is significant ($p < 0.05$), and quadratic terms of the three variables are very significant ($p < 0.01$). The Model F value of 23.02 implies the model is significant. There is only a 0.01% chance that a "Model F value" this large could occur due to noise. The "Lack of Fit F value" of 2.70 implies the Lack of Fit is not significantly relative to the pure error. There is a 15.02% chance that a "Lack of Fit F value" this large could occur due to noise. Nonsignificant lack of fit is good, and we want the model to fit.

3.2. Graphical Interpretation of the Response Surface Models. In order to determine the effect of the independent variables on the yield of biocrude, a three-dimensional diagram and contour plot for each response were generated as a function of two variables, while the other one variable was held constant. Figure 3 shows the response surface and contour plots for biocrude yield as a function of concentration (x_1) and temperature (x_2) with a holding time of 40 min. As can be seen from Figure 3, with the increase of temperature, the yield increases and finally tends towards stability. The yield

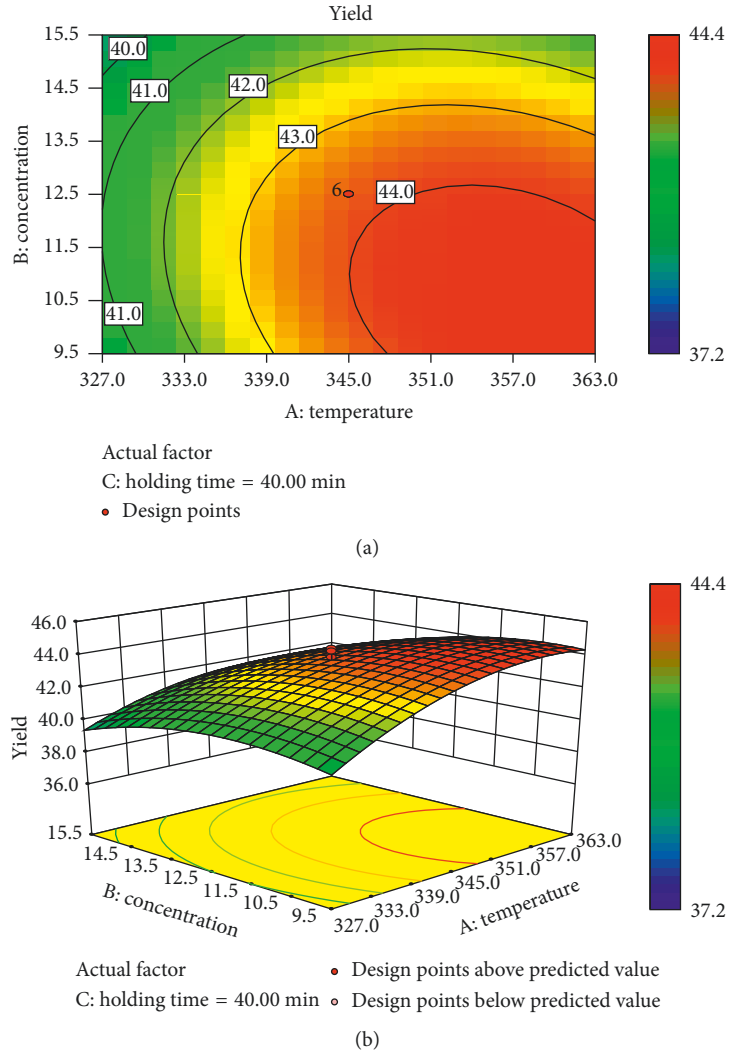

Figure 3: Contour plot and response surface plot of biocrude yield as function of temperature and concentration.

firstly increases and then decreases with the increase of the concentration. The highest yield (44.4%) occurs when the concentration and temperature are kept at about 10.5% and 355°C, respectively.

Figure 4 shows the response surface and contour plots for biocrude yield as a function of temperature (x_2) and holding time (x_3) with the concentration of 12.5%. Under this condition, the yield firstly increases and then decreases with the increase of temperature or holding time. The yield reaches to the highest (44.4%) when the concentration and holding time are kept at about 354°C and 38.5 min, respectively.

Figure 5 illustrates the response surface and contour plots for bio-oil yield as a function of concentration (x_1) and holding time (x_3) with specific temperature. The yield also shows increase at the beginning and then decrease with the increase of concentration or holding time with the temperature of 345°C. The highest yield is 44.4% when the concentration and holding time are kept at about 11% and 38 min, respectively.

3.3. Determination of HTL Process of Fresh Spirulina sp. with Optimal Variables. According to the software optimization step, the desired goal for each operational condition (temperature, holding time, and concentration) was chosen "within the range," while the response (the yield of biocrude) was defined as "maximum" to achieve the highest performance. The program combines the individual desirability into a single number and then searches to maximize this function. Accordingly, optimum working conditions are concentration of 10.5%, temperature of 357°C, and holding time of 37 min. The largest yield is 44.4%. In order to verify the optimal condition, we used cultured microalgae for the further experiment. The moisture of fresh microalgae was 82.1 ± 1.6% after centrifugation. We added some water to the microalgae slurry for the HTL process. The result of three replicated experiments was 41.6 ± 2.2%. The result indicated that when each of the parameters was set as the optimum value, the bio-oil yield was in agreement with the value predicted by the model. It implies that the strategy to optimize the HTL conditions using

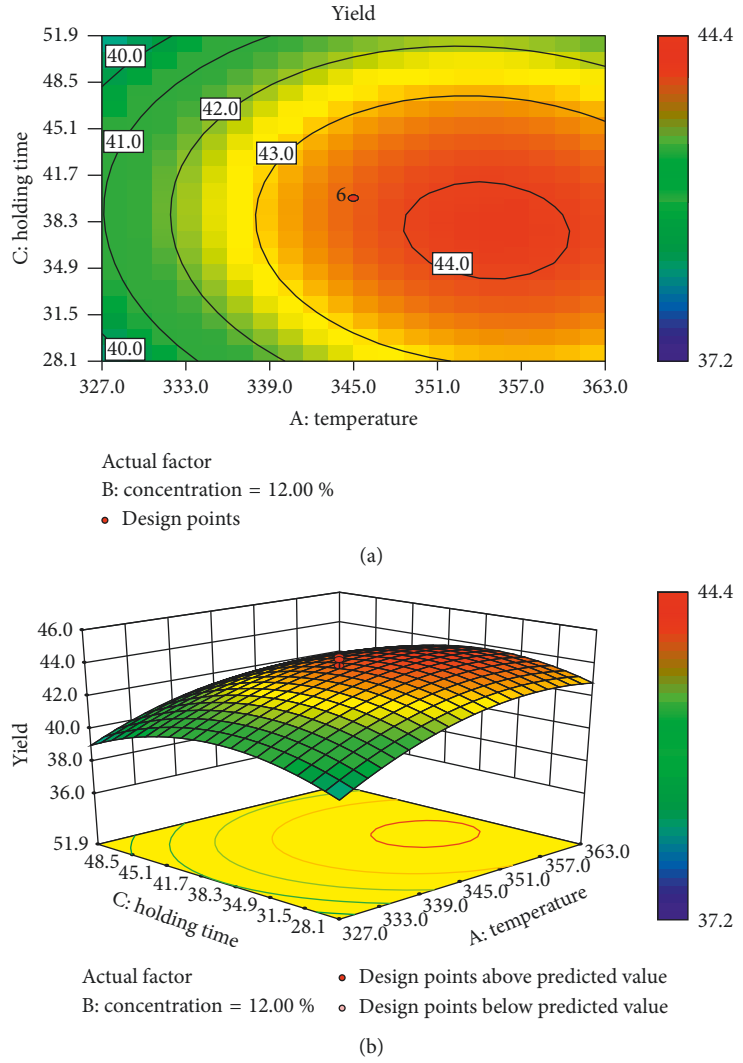

Figure 4: Contour plot and response surface plot of biocrude yield as function of temperature and holding time.

Spirulina sp. and to obtain the maximal biocrude yield by RSM in this study is feasible. Dimitriadis and Bezergianni showed that the yields from algae by HTL obtained from the literature are more dispersed, but 40% of them render a 45% oil yield [26]. Our results indicated that the biocrude yield of *Spirulina* sp. is a little less than that of some microalgae by HTL, but the performance is not bad, and it is still worth for further analysis.

3.4. FT-IR Analysis. The FT-IR analysis of bio-oil provided results consistent with the GC-MS characterization and the elemental analysis. In the FT-IR analysis, the curves (Figure 6) of the bio-oil obtained under different condition showed some difference. But most of them are similar, suggesting that the same types of functional groups exist in these samples. The composition of the bio-oil is complex as there are many absorbance band and some main bands are shown in Table 6. The bio-oil showed a strong absorbance between 2850 and 3000 cm^{-1}, indicating a high content of methyl and methylene groups. There was also a strong absorbance around between 1500 and 1700 cm^{-1}, and C=O stretching indicated the presence of ketones, aldehydes, esters, or acids.

3.5. GC-MS Analysis. Specific compositions of the biocrude products were not easily identifiable by FT-IR, so the biocrude obtained from fresh *Spirulina* sp. by the HTL was characterized by GC-MS for identification of their chemical compositions too. For a better understanding of the properties of the biocrude, a mass spectral library and computer matching were used to facilitate compound identification. Hundreds of peaks were detected by GC-MS in this investigation. The results reveal that the HTL-based microalgal biocrude is an extremely complex mixture of numerous compounds; some major chemical categories are listed in Table 7. The compositions are far different from the bio-oil obtained from the *Chlorella pyrenoidosa* or *Dunaliella tertiolecta* cake by HTL [27–29]. Some compounds are similar

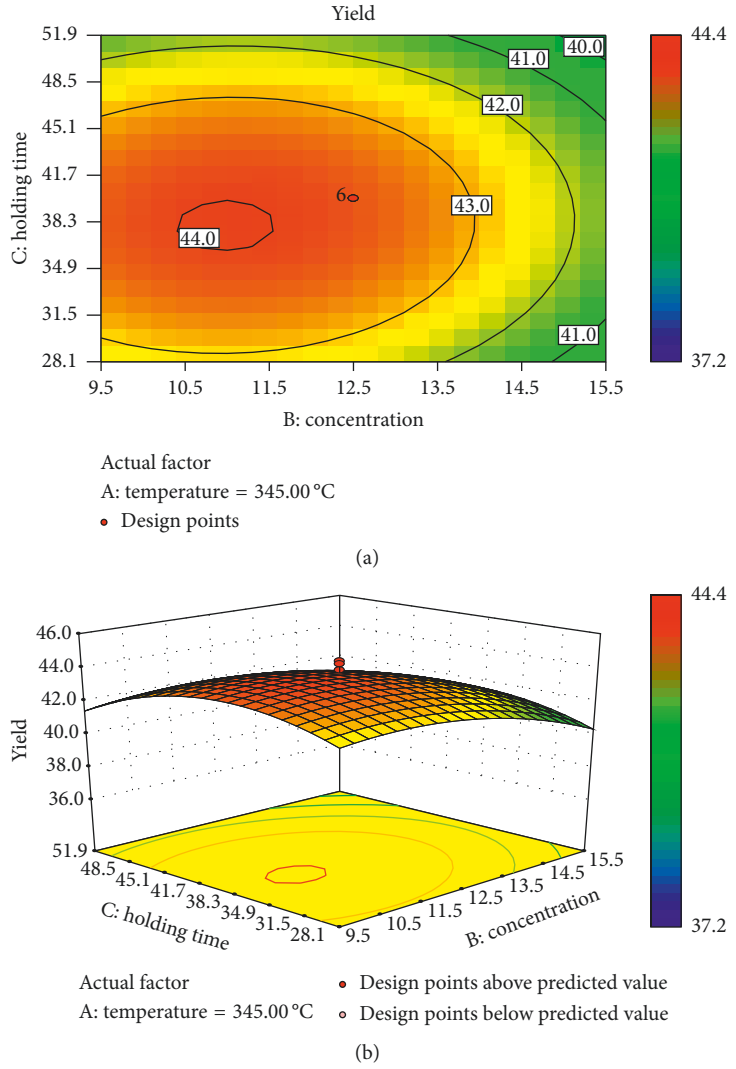

Figure 5: Contour plot and response surface plot of biocrude yield as function of holding time and concentration.

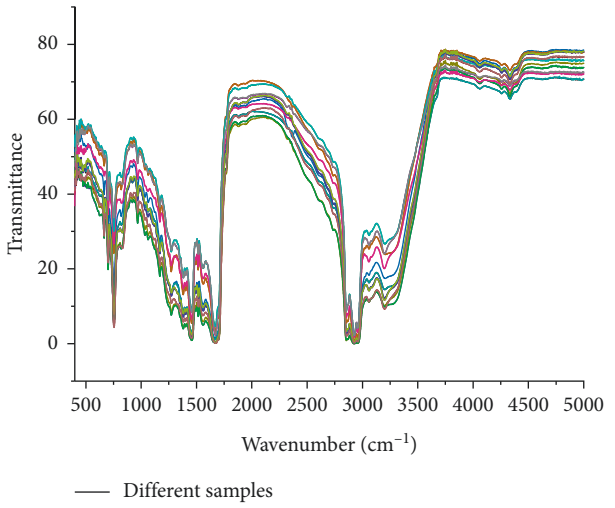

Figure 6: FT-IR spectra of bio-oil from hydrothermal liquefaction of *Spirulina* sp. powder under different conditions.

with the compounds in bio-oil obtained by hydrothermal liquefaction of *Chlorella vulgaris* and *Spirulina* using alkali and organic acids as catalyst [20, 30]. The final hydrocarbon product has about 19 wt.% in naphtha range (mainly C_5–C_{10}) and 84 wt.% in diesel range (mainly C_{10}–C_{20}). The hydrocarbons have about 7 wt.% larger than C_{20}. That is probably why the biocrude was a dark viscous liquid.

4. Conclusion

In this study, bio-oil crude was produced by hydrothermal liquefaction using *Spirulina* sp. By RSM optimization, we got the optimal reactor condition that was 10.5% of concentration, 37 min of holding time, and 357°C of temperature and finally got the yield of 41.6 ± 2.2% using the fresh *Spirulina* sp. as the feedstock. Among the three variables examined in this study, temperature and concentration were the most influential factors on the product oil yield. The characteristic of the bio-crude displayed the potential

Table 6: The main FT-IR function group composition of biocrude from HTL of *Spirulina* sp.

Frequency range cm^{-1}	Frequency cm^{-1}	Assignment
550–450	537	S–S stretching
750–650	617, 697, 745	Secondary amid N–H wagging
915–650	835, 903	O–H bending
965–930	962	Oxime N–O stretching
1,060–1,020	1,025	S=O stretching
1,070–1,050	1,064	CH_2 twisting
1,300–1,100	1,151, 1,177	C–O stretching
1,370–1,330	1,365	Aromatic nitro compound NO_2 symmetric stretching
1,400–1,450	1,448	Azo compound N≡N stretching
1,540–1,500	1,490	Aromatic nitro compound NO_2 asymmetric stretching
1,560–1,530	1,535	Secondary amide N–H bending, C–N stretching
1,615–1,565	1,598	Pyridine C–N stretching, C=C stretching
1,640–1,680	1,662	Primary and secondary amide C=O stretching
2,130–2,100	2,102	Aromatic isonitrile–N–C stretching
2,180–2,110	2,186	Aliphatic isonitile-N–C stretching
3,000–2,800	2,846, 2,909	$C–H_3$ stretching
3,105–3,000	3,019, 3,066, 3,051	CH_2 stretching
3,190–3,170	3,179	Primary amide NH_2 symmetric stretching

Table 7: Major chemical compositions of bio-oil from hydrothermal liquefaction of fresh *Spirulina* sp. biomass at the concentration of 10.5%, temperature of 357°C, and holding time of 37 min.

Number	RT (min)	Name of compounds	Molecular formula	Area (%)
1	15.95	Octane, 2,4,6-trimethyl	$C_{19}H_{40}$	2.78
2	19.84	1,2-Bis(benzoyloxy) benzene	$C_{20}H_{18}O_2$	2.81
3	29.97	Eicosane	$C_{20}H_{42}$	1.71
4	23.51	Decane, 3-ethyl-3-methyl	$C_{18}H_{38}$	1.98
5	24.07	Octane, 5-ethyl-2-methyl	$C_{19}H_{40}$	2.54
6	31.01	Hexacosane	$C_{26}H_{54}$	2.46
7	31.52	Phenol, 2,4-bis(1,1-dimethylethyl)	$C_{14}H_{22}O$	2.90
8	36.85	Heptadecane	$C_{17}H_{36}$	3.17
9	40.06	Naphthalene, 2,7-dimethyl	$C_{13}H_{23}NO_4$	4.11
10	44.33	Hexadecanoic acid, ethyl ester	$C_{18}H_{36}O_2$	1.67

ability of *Spirulina* sp. to be a valuable and environmentally friendly feedstock candidate for biofuels and biochemicals. As some of the compounds in biocrude, such as fatty acids and aldehydes, are directly related to the undesirable properties of bio-oil, the biocrude still needs more improvement to be used as the liquid fuel.

Conflicts of Interest

The authors declare that they have no conflicts of interest.

Acknowledgments

This study was supported by the Natural Science Foundation of Fujian (2017J05041) and Fundamental Research Funds for the Central Universities. The authors thank the project of Gaoyuan Agricultural Engineering of Fujian (712018014).

References

[1] P. Ayala-Parra, Y. Liu, J. A. Field, and R. Sierra-Alvarez, "Nutrient recovery and biogas generation from the anaerobic digestion of waste biomass from algal biofuel production," *Renewable Energy*, vol. 108, pp. 410–416, 2017.

[2] P. Schenk, S. R. Thomas-Hall, E. Stephens et al., "Second generation biofuels: high-efficiency microalgae for biodiesel production," *BioEnergy Research*, vol. 1, no. 1, pp. 20–43, 2008.

[3] P. Singh, S. Kumari, A. Guldhe, R. Misra, I. Rawat, and F. Bux, "Trends and novel strategies for enhancing lipid accumulation and quality in microalgae," *Renewable and Sustainable Energy Reviews*, vol. 55, pp. 1–16, 2016.

[4] A. Bahadar and M. B. Khan, "Progress in energy from microalgae: a review," *Renewable and Sustainable Energy Reviews*, vol. 27, pp. 128–148, 2013.

[5] K. Y. Show and D. J. Lee, "Chapter 9-production of biohydrogen from microalgae," in *Biofuels from Algae*, A. Pandey, D. J. Lee, Y. Chisti, and C. R. Soccol, Eds., pp. 189–204, Elsevier, Amsterdam, Netherlands, 2014.

[6] S. B. Velasquez-Orta, J. G. M. Lee, and A. P. Harvey, "Evaluation of FAME production from wet marine and freshwater microalgae by *in situ* transesterification," *Biochemical Engineering Journal*, vol. 76, pp. 83–89, 2013.

[7] J. C. Frigon, F. Matteau-Lebrun, R. Hamani Abdou, P. J. McGinn, S. J. B. O'Leary, and S. R. Guiot, "Screening microalgae strains for their productivity in methane following anaerobic digestion," *Applied Energy*, vol. 108, pp. 100–107, 2013.

[8] Y. Peralta-Ruíz, Y. Pardo, S. González-Delgado, and V. Kafarov, "Simulation of bioethanol production process from residual microalgae biomass," in *Computer Aided Chemical Engineering*, B. Ian David Lockhart and F. Michael, Eds., vol. 30, pp. 1048–1052, Elsevier, Amsterdam, Netherlands, 2012.

[9] P. J. Valdez, M. C. Nelson, H. Y. Wang, X. N. Lin, and P. E. Savage, "Hydrothermal liquefaction of *Nannochloropsis* sp.: systematic study of process variables and analysis of the product fractions," *Biomass and Bioenergy*, vol. 46, pp. 317–331, 2012.

[10] G. Yu, Y. Zhang, L. Schideman, T. Funk, and Z. Wang, "Distributions of carbon and nitrogen in the products from hydrothermal liquefaction of low-lipid microalgae," *Energy and Environmental Science*, vol. 4, no. 11, pp. 4587–4595, 2011.

[11] C. Yusuf, "Biodiesel from microalgae," *Biotechnology Advances*, vol. 25, no. 3, pp. 294–306, 2007.

[12] P. Biller, R. Riley, and A. B. Ross, "Catalytic hydrothermal processing of microalgae: Decomposition and upgrading of lipids," *Bioresource Technology*, vol. 102, no. 7, pp. 4841–4848, 2011.

[13] A. Marcilla, L. Catalá, J. C. García-Quesada, F. J. Valdés, and M. R. Hernández, "A review of thermochemical conversion of microalgae," *Renewable and Sustainable Energy Reviews*, vol. 27, pp. 11–19, 2013.

[14] Y. Hu, M. Gong, C. Xu, and A. Bassi, "Investigation of an alternative cell disruption approach for improving hydrothermal liquefaction of microalgae," *Fuel*, vol. 197, pp. 138–144, 2017.

[15] D. L. Barreiro, B. R. Gómez, F. Ronsse, U. Hornung, A. Kruse, and W. Prins, "Heterogeneous catalytic upgrading of biocrude oil produced by hydrothermal liquefaction of microalgae: state of the art and own experiments," *Fuel Processing Technology*, vol. 148, pp. 117–127, 2016.

[16] X. Wang, L. Sheng, and X. Yang, "Pyrolysis characteristics and pathways of protein, lipid and carbohydrate isolated from microalgae *Nannochloropsis* sp," *Bioresource Technology*, vol. 229, pp. 119–125, 2017.

[17] D. M. Li and Y. Z. Qi, "*Spirulina* industry in China: present status and future prospects," *Journal of Applied Phycology*, vol. 9, no. 1, pp. 25–28, 1997.

[18] Y. M. Lu, W. Z. Xiang, and Y. H. Wen, "*Spirulina* (Arthrospira) industry in Inner Mongolia of China: current status and prospects," *Journal of Applied Phycology*, vol. 23, no. 2, pp. 265–269, 2011.

[19] H. J. Huang, X. Z. Yuan, H. N. Zhu et al., "Comparative studies of thermochemical liquefaction characteristics of microalgae, lignocellulosic biomass and sewage sludge," *Energy*, vol. 56, pp. 52–60, 2013.

[20] A. B. Ross, P. Biller, M. L. Kubacki, H. Li, A. Lea-Langton, and J. M. Jones, "Hydrothermal processing of microalgae using alkali and organic acids," *Fuel*, vol. 89, no. 9, pp. 2234–2243, 2010.

[21] C. Jazrawi, P. Biller, A. B. Ross, A. Montoya, T. Maschmeyer, and B. S. Haynes, "Pilot plant testing of continuous hydrothermal liquefaction of microalgae," *Algal Research*, vol. 2, no. 3, pp. 268–277, 2013.

[22] Y. Elkasabi, B. M. E. Chagas, C. A. Mullen, and A. A. Boateng, "Hydrocarbons from *Spirulina* pyrolysis bio-oil using one-step hydrotreating and aqueous extraction of heteroatom compounds," *Energy & Fuels*, vol. 30, no. 6, pp. 4925–4932, 2016.

[23] D. Beckman, *Techno-Economic Assessment of Selected Biomass Liquefaction Processes*, VTT Technical Research Centre of Finland, Espoo, Finland, 1990.

[24] S. A. Channiwala and P. P. Parikh, "A unified correlation for estimating HHV of solid, liquid and gaseous fuels," *Fuel*, vol. 81, no. 8, pp. 1051–1063, 2002.

[25] C. Sheng and J. L. T. Azevedo, "Estimating the higher heating value of biomass fuels from basic analysis data," *Biomass and Bioenergy*, vol. 28, no. 5, pp. 499–507, 2005.

[26] A. Dimitriadis and S. Bezergianni, "Hydrothermal liquefaction of various biomass and waste feedstocks for biocrude production: a state of the art review," *Renewable and Sustainable Energy Reviews*, vol. 68, pp. 113–125, 2017.

[27] Z. Shuping, W. Yulong, Y. Mingde, I. Kaleem, L. Chun, and J. M. Tong, "Production and characterization of bio-oil from hydrothermal liquefaction of microalgae Dunaliella tertiolecta cake," *Energy*, vol. 35, no. 12, pp. 5406–5411, 2010.

[28] P. Duan, B. Jin, Y. Xu et al., "Thermo-chemical conversion of *Chlorella pyrenoidosa* to liquid biofuels," *Bioresource Technology*, vol. 133, pp. 197–205, 2013.

[29] J. Zhang, W. T. Chen, P. Zhang, Z. Luo, and Y. Zhang, "Hydrothermal liquefaction of *Chlorella pyrenoidosa* in sub- and supercritical ethanol with heterogeneous catalysts," *Bioresource Technology*, vol. 133, pp. 389–397, 2013.

[30] U. Jena and K. C. Das, "Comparative evaluation of thermochemical liquefaction and pyrolysis for bio-oil production from microalgae," *Energy & Fuels*, vol. 25, no. 11, pp. 5472–5482, 2011.